

Classification of N^{13} Levels by Partial Wave Analysis of Proton Scattering from C^{12*}

HERBERT L. JACKSON† AND AARON I. GALONSKY
University of Wisconsin, Madison, Wisconsin

(Received July 19, 1951)

The nature of the excited levels in N^{13} between 2.24 and 5.64 Mev was investigated by analyzing the $C^{12}(p,p)C^{12}$ data of Goldhaber and Williamson. To carry out the analysis, the partial wave phase shifts were related to the level parameters by means of one level dispersion theory. Then by successive approximations of the level parameters, the partial wave expansion of the differential cross section for elastic scattering was fitted to the experimental curve. The analysis leads to the conclusion that the lower scattering anomaly is due to an $S_{\frac{1}{2}}$ level at 2.379 Mev above the ground state, and that the higher scattering anomaly results from a $P_{\frac{3}{2}}$ level at 3.501 Mev and a $D_{\frac{3}{2}}$ level at 3.549 Mev. Neither experiment nor analysis indicates any other levels in the range considered. It is shown that no other simple level assignment can account for the observed scattering cross section. The appearance of levels with $j=l+\frac{1}{2}$ instead of $j=l-\frac{1}{2}$ supports Mayer's hypothesis of level inversion in nuclei. The widths and energies of the levels obtained from the present analysis are in partial agreement with the values obtained from the (p,γ) reaction.

I. INTRODUCTION

THE low-lying energy levels of the N^{13} nucleus are currently of particular interest. For one reason, N^{13} is the mirror of C^{13} , whose levels have been observed. If the pp and nn forces are equal, the energy levels of mirror pairs such as C^{13} and N^{13} should have the same quantum numbers and similar reduced widths and characteristic energies. Thus knowledge of the energy level schemes of such nuclei will contribute toward an understanding of nuclear forces. Moreover, the level scheme of N^{13} should be fairly simple to interpret because, according to the closed shell model, this nucleus consists of a core of closed neutron and proton shells plus one outer proton. Finally, N^{13} is especially suitable for study by elastic proton scattering because: (1) its ground state is only 1.945 ± 0.004 Mev below the dissociation energy,¹ (2) the scattering nucleus C^{12} has zero spin, and (3) no other process competes seriously below 5.6 Mev. Thus, an unusually low-energy range is available for this kind of experiment, and the results are relatively easy to analyze since j can have only the values $l \pm \frac{1}{2}$.

Goldhaber and Williamson² obtained the $C^{12}(p,p)C^{12}$ differential cross section at a laboratory angle of 164° for bombarding energies extending from 0.32 to 4.00 Mev. Their results show two prominent scattering anomalies with maxima at 0.484 and 1.73 Mev. For convenience these anomalies are hereafter called resonances as distinct from the energy levels causing them. In order to determine the nature of the levels giving rise to these resonances, the partial wave expansion of the differential cross section for elastic proton scattering was fitted to Goldhaber's and Williamson's data. For

spinless nuclei this expansion assumes the form:³

$$\frac{d\sigma}{d\omega} = \frac{1}{k^2} \left| -\frac{1}{2} \eta \csc^2 \frac{\theta}{2} \exp i\eta \ln \csc^2 \frac{\theta}{2} + \sum_{l=0}^{\infty} [(l+1) \sin \delta_l^+ \exp i\delta_l^+ + l \sin \delta_l^- \exp i\delta_l^-] \times P_l(\cos \theta) \exp i\alpha_l \right|^2 + \frac{\sin^2 \theta}{k^2} \left| \sum_{l=1}^{\infty} (\sin \delta_l^+ \exp i\delta_l^+ - \sin \delta_l^- \exp i\delta_l^-) P_l'(\cos \theta) \exp i\alpha_l \right|^2,$$

where $d\sigma/d\omega$ is the differential cross section in the center-of-mass coordinate system; $k=1/\lambda=\mu v/\hbar$, μ being the reduced mass of the proton and v , its initial velocity; $\eta=ZZ'e^2/\hbar v$; δ_l^\pm is the noncoulomb phase shift of the partial wave of orbital angular momentum l and total angular momentum $j=l \pm \frac{1}{2}$;

$$e^{i\alpha_l} = \prod_{s=1}^l \left(\frac{s+i\eta}{s-i\eta} \right) \text{ for } l > 0, \text{ and } e^{i\alpha_0} = 1;$$

θ is the scattering angle in the center-of-mass coordinate system; $P_l(\cos \theta)$ is the l th Legendre polynomial; and $P_l'(\cos \theta)$ is the first derivative of $P_l(\cos \theta)$ with respect to its argument, $\cos \theta$. The first squared expression of the expansion represents those protons whose spins do not change direction in the scattering process, while the second squared expression represents those protons whose spins have been reversed.³ Thus, the first expression gives the coherent part of the scattering and the second, the incoherent part.

The expansion of $d\sigma/d\omega$ is useful only if the phase shifts can be related to parameters characteristic of the levels involved. To connect δ_l^\pm with the desired level parameters we adopt the two following assumptions: (1) Elastic scattering is by far the most probable

* Supported by the Wisconsin Alumni Research Foundation and the AEC.

† Kimberly-Clark Fellow.

¹ Calculated from the Q value of the $C^{12}(d,n)N^{13}$ reaction of Bonner, Evans, and Hill, Phys. Rev. **75**, 1398 (1949), and the deuteron binding energy of R. C. Mobley and R. A. Laubenstein, Phys. Rev. **80**, 309 (1950).

² Gerson Goldhaber and R. M. Williamson, Phys. Rev. **82**, 495 (1951).

³ This result follows immediately from Eqs. (4) and (5), C. L. Critchfield and D. C. Dodder, Phys. Rev. **76**, 602 (1949).

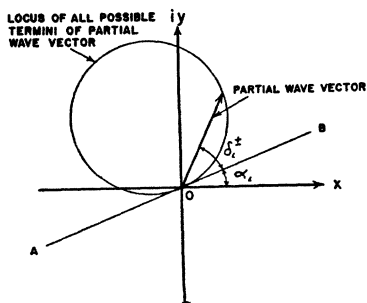


FIG. 1. Graphical representation of the dependence of the scattering amplitude of the (l, j) th partial wave on the phase shift δ_l^\pm . Since the scattering amplitude is a complex number, it may be treated as a two-dimensional vector. As δ_l^\pm increases from 0° to 180° , the head of the vector traces out a circle in the complex plane. This circle is of diameter $j + \frac{1}{2}$ units, touches the origin, and is inclined at an angle α_l (see text) to the real axis. The superscript \pm signifies that $j = l \pm \frac{1}{2}$.

process for each of the levels to be investigated. (2) Each of the observed scattering anomalies appreciably involves only one level of given angular momentum and parity. This assumption is, of course, the one-level approximation.

In the case of N^{13} these conditions are reasonably fulfilled. The only process present other than the elastic scattering is the (p, γ) reaction, and both the (p, p) and the (p, γ) data indicate a very simple level scheme up to 5.64 Mev. On the basis of the above assumptions the formalism of Wigner and Eisenbud⁴ leads to the following simple expression for the partial wave phase shifts:⁵

$$\delta_l^\pm = -\arctan(F_l/G_l)_a + \arctan\left[\frac{1}{2}\Gamma_\lambda/(E_\lambda + \Delta_\lambda - E)\right]_a.$$

The first term on the right-hand side is usually called the potential phase shift, and the second, the resonant phase shift. The quantities F_l and G_l are the regular and irregular radial coulomb wave functions, respectively.⁶ These quantities are functions of $\rho = kr$ and η , and must be evaluated for a chosen interaction radius, $r = a$. The second term depends on the interaction radius a , the incident proton energy E , and two parameters characteristic of the level. These parameters are the reduced width γ_λ^2 , and the characteristic energy E_λ , which is closely related to the resonant energy E_r . Both E_λ and γ_λ^2 are independent of the momentum of the incident particle. By definition, the resonant energy E_r is that value of E for which $\delta_l^\pm = 90^\circ$. For low energies or high angular momenta E_r is also very nearly that value of E for which $E_\lambda + \Delta_\lambda - E = 0$. The subscript λ signifies the various quantum numbers of the level. The relation between the experimental and reduced width⁴ is

$$\frac{1}{2}\Gamma_\lambda = (k\gamma_\lambda^2/A_l^2)_a$$

⁴ E. P. Wigner and L. Eisenbud, Phys. Rev. **72**, 29 (1947).

⁵ R. K. Adair, private communication.

⁶ Bloch, Hull, Jr., Broyles, Bouricius, Freeman, and Breit, Revs. Modern Phys. **23**, 147 (1951).

where $A_l^2 = F_l^2 + G_l^2$, and

$$\Delta_\lambda = -\left[\frac{k\gamma_\lambda^2}{\rho} \left(\frac{\rho}{A_l} \frac{dA_l}{d\rho} + l\right)\right]_{\rho=ka}.$$

Since the arguments of the arctangents are dimensionless, and since all the quantities entering the argument of the resonance term have the dimension of energy, each quantity may be calculated either in the center-of-mass or laboratory system of coordinates, and E_λ and E may be measured from any convenient zero point. Throughout this paper E_λ , E , E_r , and γ_λ^2 are given their center-of-mass values, with the ground state of N^{13} as the energy zero, while E_p signifies the initial kinetic energy of the incident proton in the laboratory system.

II. METHOD

The analysis must begin with a choice of the parameter a because it determines the values of the coulomb wave functions and the quantities derived from them. In the formalism of Wigner and Eisenbud⁴ the quantity a is completely arbitrary, except for a lower limit such that for all $r > a$, the interaction of the proton and target nucleus can be represented by a potential. However, in the one level approximation, it is advantageous to choose a as small as possible; that is, equal to the range of the noncoulomb interaction. Although the most suitable choice of a is somewhat indefinite, the value

$$a = 1.45((A)^{\frac{1}{3}} + (1)^{\frac{1}{3}}) \times 10^{-13} \text{ cm}$$

suggested by Ehrman,⁷ which is the sum of the radii of the proton and the target nucleus, was used throughout this analysis and seems satisfactory. Once a has been chosen, the analysis consists essentially of choosing those values of j , l , E_λ , and γ_λ^2 which best fit the experimental data. l and j are found by trial and error and E_λ and γ_λ^2 by successive approximation. The simplest technique is the graphical treatment worked out by Laubenstein.⁸ Momentarily ignoring the factor $1/k$, one can write the amplitude of the coherent scattering thus:

$$-\frac{1}{2}\eta \csc^2 \frac{1}{2}\theta \exp(i\eta \ln \csc^2 \frac{1}{2}\theta) + \sin \delta_0 \exp(i\delta_0) \\ + P_1(\cos \theta) \sin \delta_1^- \exp(i\delta_1^- + i\alpha_1) \\ + 2P_1(\cos \theta) \sin \delta_1^+ \exp(i\delta_1^+ + i\alpha_1) + \dots$$

This is a sum of complex numbers, each specified by its modulus and phase. The first term represents the Rutherford scattering; the second, that due to the $S_{\frac{1}{2}}$ phase shift, and so on. It is most informative to treat the terms as two-dimensional vectors in the complex plane, adding them by the closed polygon method. The coherent scattering cross section is then simply the absolute square of the resultant times $1/k^2$. For simplicity, the successive terms are called the Rutherford or R vector, the $S_{\frac{1}{2}}$ vector, the $P_{\frac{1}{2}}$ vector, and so on.

⁷ J. B. Ehrman, Phys. Rev. **81**, 412 (1951).

⁸ R. A. Laubenstein, Ph.D. thesis, University of Wisconsin, 1950.

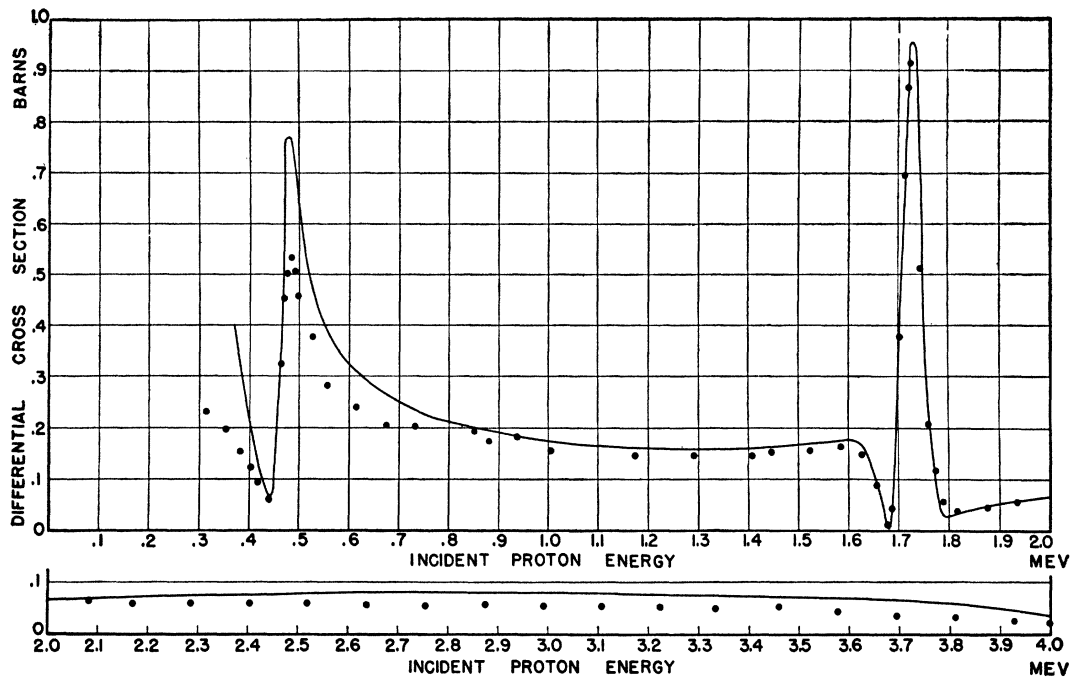


FIG. 2. Comparison of the experimental and calculated $C^{12}(p,p)C^{12}$ cross section from 0.32 to 4.0 Mev. The curve was calculated from the parameters given in Table I. The points are from Goldhaber's and Williamson's experimental data.

The partial wave vectors have other useful properties. As δ_l^\pm goes from 0° to 180° , the head of the associated vector describes a circle of diameter $(j + \frac{1}{2})P_l$ in the complex plane (see Fig. 1). This circle touches the origin (the point of contact corresponding to $\delta_l^\pm = 0^\circ$ or 180°), and is tangent to a line AB which passes through the origin and makes an angle α_l with the real axis. As δ_l^\pm increases, the head of the vector travels counterclockwise. The various circles, which are the loci of all possible end points of their corresponding vectors will henceforth be called the $S_{\frac{1}{2}}$ circle, the $P_{\frac{1}{2}}$ circle, and so on. Similar considerations apply to the incoherent scattering. Since this part of the scattering is proportional to $\sin^2\theta$, it is usually unimportant for scattering angles near 180° . In the present case, calculation shows that it is negligible except near the maximum of the upper resonance. Since the expansion of $d\sigma/d\omega$ depends only upon the kinematics of the scattering process, these properties of the partial wave vectors are independent of the simplifying assumptions introduced to get an analytic expression for δ_l^\pm . From the above-discussed behavior of the scattering terms it is easy to predict the shape of any single narrow resonance if it is assumed that the other vectors contributing to the scattering change but little in the region of interest. Such is the case in the one-level approximation. Broad or overlapping levels are more difficult to analyze and require special effort to establish the uniqueness of the fit.

III. RESULTS

To fit the experimental cross section it is necessary to assign the lower resonance to an $S_{\frac{1}{2}}$ level and the

higher resonance to a $P_{\frac{1}{2}}$ and $D_{\frac{1}{2}}$ level closely spaced. The letters S , P , and D designate the orbital angular momentum of the incident proton exciting the level, and hence specify the parity of the level itself. Insofar as the nucleus is accurately described by the single particle model, these letters also give the orbital momentum of the outermost proton. The numerical values of the level parameters which yield the best fit of the data thus far obtained are given in Table I. The widths Γ were determined from plots of the (p,γ) cross section which were calculated for the values of E_λ and γ_λ^2 given in the table. Figure 2 shows the cross section curve calculated from the values in Table I together with a number of experimental points to show the agreement. The incoherent contribution to the scattering has been included and amounts to about 10 percent of the total at the peak of the upper resonance. In Fig. 2 the experimental points fall considerably below the calculated curve for energies less than 0.8 Mev. At the lower resonance the potential phase shifts are approximately zero for all l , so that the calculated maximum and minimum of that resonance depend only on the R vector and the diameter of the $S_{\frac{1}{2}}$ circle, both of which are independent of the interaction radius and hence unambiguous. It is therefore suspected that the disagreement results from poor experimental counting efficiency in this range.

The scattered protons were detected with a zinc sulfide scintillation counter which compared favorably with a proportional counter above one Mev. It was not feasible to check its performance at lower energies.² However, examination of the counter output with an

TABLE I. Parameters of the excited levels in N^{13} . The reduced width γ_λ^2 and characteristic energy E_λ are parameters appearing in the dispersion theory formalism. E_r is the resonant energy of the level and Γ is its width at half-maximum. All values in the table are computed in the center-of-mass system, and E_λ and E_r are measured from the ground state of N^{13} , which is taken to be 1.945 Mev below the C^{12} , p dissociation energy.

Level	γ_λ^2 (Mev cm)	E_λ (Mev)	Γ (Mev)	E_r (Mev)
$S_{\frac{1}{2}}$	7.565×10^{-13}	0.980	0.033	2.379
$P_{\frac{1}{2}}$	0.3766×10^{-13}	3.508	0.042	3.501
$D_{\frac{1}{2}}$	2.356×10^{-13}	3.593	0.040	3.549

oscilloscope showed a wide variation of pulse height. As it was necessary to use a discriminator to remove the gamma-ray pulses, quite possibly many low-energy proton pulses were missed, thus lowering this portion of the experimental curve.

To be convincing, the level assignment must be unique. It is therefore necessary not only to obtain a reasonable fit of the experimental data, but also to eliminate all other possibilities. Earlier investigators⁹ have interpreted the first resonance as an $S_{\frac{1}{2}}$ level. The present fit, therefore, confirms the previous assignment. The upper resonance requires more thorough discussion. It is evident from Fig. 2 that the most informative part of the resonance lies between $E_p=1.65$ and 1.85 Mev. The crucial features of the curve are: (a) the slight rise of the curve below 1.68 Mev, (b) the very small magnitude of the minimum at 1.68 Mev, (c) the high maximum at 1.73 Mev, and (d) the shallow minimum at 1.83 Mev. Any believable level assignment must explain all these properties. In this range the R vector and the potential phase shifts are nearly constant. In addition, the potential phase shifts, $-\arctan F_l/G_l$, are nearly zero for $l > 1$, so all D and higher terms not containing a resonance vanish. Wigner's criterion⁴ rules out the possibility of any resonance with $l \geq 3$. For $a=4.77 \times 10^{-13}$ cm,

$$\gamma_\lambda^2 \leq 3\hbar^2/2\mu a \doteq 14 \times 10^{-13} \text{ Mev cm},$$

but for an experimental width of 40 kev and $l=3$,

$$\gamma_\lambda^2 = \Gamma_\lambda A_3^2/2k \doteq 32 \times 10^{-13} \text{ Mev cm}$$

which is over two times too large. Since for a given ρ and η , A_l increases with l , all resonances of higher orbital angular momentum are also excluded. A smaller value of a yields a larger limit, but also a much larger value for A_l^2 , so the argument remains valid.

It is easy to show that no single S , P , or D level will account for the experimental shape. This is most simply done by drawing suitable vector diagrams, giving all nonresonance vectors their values at $E_p \sim 1.7$ Mev and replacing the assumed resonant vector with its corresponding circle. The incoherent scattering is ignored since its only effect is to increase the maximum slightly. Figure 3 shows each possibility. From these diagrams it

⁹ For bibliography see Hornyak, Lauritsen, Morrison, and Fowler, *Revs. Modern Phys.* **22**, 291 (1950).

is clear that an $S_{\frac{1}{2}}$, $P_{\frac{1}{2}}$, $D_{\frac{1}{2}}$, or $D_{\frac{3}{2}}$ level cannot produce the small minimum since the corresponding circle does not pass near the origin. Although a $P_{\frac{1}{2}}$ level will produce the small minimum, the $P_{\frac{1}{2}}$ circle is so situated that the maximum resultant is very little larger than the sum of the nonresonant R , $S_{\frac{1}{2}}$, and $P_{\frac{1}{2}}$ vectors alone so that the high maximum at $E_p=1.73$ Mev is unattainable. Hence, the observed resonance cannot be due to any single level.

The next simplest assumption is that the resonance is due to two closely spaced levels. As the objection to F or higher levels still holds, the possible combinations are

$$\begin{array}{lllll} S_{\frac{1}{2}}S_{\frac{1}{2}} & P_{\frac{1}{2}}P_{\frac{1}{2}} & P_{\frac{1}{2}}P_{\frac{3}{2}} & D_{\frac{1}{2}}D_{\frac{1}{2}} & D_{\frac{1}{2}}D_{\frac{3}{2}} \\ S_{\frac{1}{2}}P_{\frac{1}{2}} & P_{\frac{1}{2}}P_{\frac{3}{2}} & P_{\frac{3}{2}}D_{\frac{1}{2}} & D_{\frac{1}{2}}D_{\frac{3}{2}} & \\ S_{\frac{1}{2}}P_{\frac{3}{2}} & P_{\frac{3}{2}}D_{\frac{1}{2}} & P_{\frac{3}{2}}D_{\frac{3}{2}} & & \\ S_{\frac{1}{2}}D_{\frac{1}{2}} & P_{\frac{1}{2}}D_{\frac{1}{2}} & & & \\ S_{\frac{1}{2}}D_{\frac{3}{2}} & & & & \end{array}$$

Each of these must be considered in detail. Obviously such combinations as $S_{\frac{1}{2}}S_{\frac{1}{2}}$ or $P_{\frac{1}{2}}P_{\frac{1}{2}}$ violate the single level approximation made earlier. However, this approximation was introduced only for the purpose of obtaining an expression for δ_{l^\pm} in terms of the level parameters and incident proton energy. Therefore, when dealing with combinations involving two levels with the same l and j , the discussion must be independent of the analytic form of δ_{l^\pm} . Fortunately, the properties of the locus circles are unchanged and are sufficient to eliminate all such combinations requiring consideration.

$S_{\frac{1}{2}}S_{\frac{1}{2}}$

The maximum cross section obtainable from this combination is

$$\begin{aligned} (d\sigma/d\omega)_{\max} &= k^{-2} |\mathbf{R} + \mathbf{P}_{\frac{1}{2}} + \mathbf{P}_{\frac{1}{2}} + \mathbf{S}_{\frac{1}{2}}|^2_{\max} \\ &\leq k^{-2} (|\mathbf{R}| + |\mathbf{P}_{\frac{1}{2}}| + |\mathbf{P}_{\frac{1}{2}}| + |\mathbf{S}_{\frac{1}{2}}|_{\max})^2 < 0.4 \text{ barn}. \end{aligned}$$

This disagrees with experiment, which gives a maximum at $E_p=1.73$ Mev of almost one barn.

$S_{\frac{1}{2}}P_{\frac{1}{2}}$ and $S_{\frac{1}{2}}P_{\frac{3}{2}}$

Figure 4 applies to the $S_{\frac{1}{2}}P_{\frac{1}{2}}$ case. The R and $P_{\frac{1}{2}}$ vectors as well as the $S_{\frac{1}{2}}$ circle are the same as in Fig. 3(a). Every point on the $S_{\frac{1}{2}}$ circle is a possible end point of the $S_{\frac{1}{2}}$ vector from which a $P_{\frac{1}{2}}$ circle may be drawn. It is easily seen that the locus of centers of all possible $P_{\frac{1}{2}}$ circles is another circle having the same radius as the $S_{\frac{1}{2}}$ circle. This is circle No. 2 in the figure. Circle No. 3 is the outer envelope of all possible $P_{\frac{1}{2}}$ circles. As no $P_{\frac{1}{2}}$ circle touches any point outside the outer envelope, the largest cross section obtainable under any circumstance is that calculated from the resultant drawn in the figure. Together with the incoherent part, which does not exceed 0.009 barn, this gives

$$(d\sigma/d\omega)_{\max} = 0.54 \text{ barn}$$

which is too small. The same argument is much stronger for the $S_{\frac{1}{2}}P_{\frac{3}{2}}$ case, because the diameter of the $P_{\frac{3}{2}}$ circle

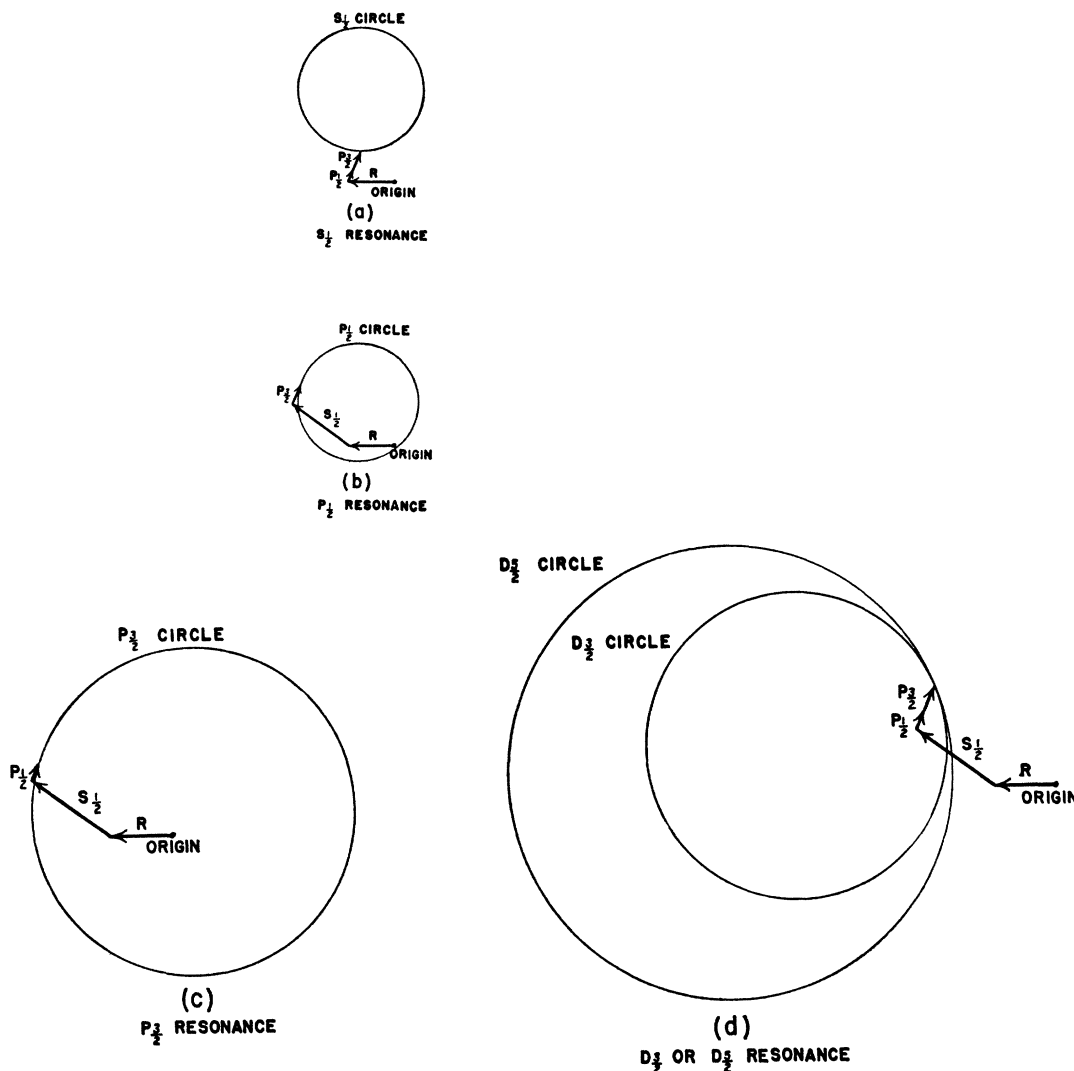


FIG. 3. The partial wave vectors at $E_p \sim 1.7$ Mev drawn on the assumption that the scattering anomaly at this energy is due to (a) an $S_{1/2}$ level, (b) a $P_{1/2}$ level, (c) a $P_{3/2}$ level, (d) a $D_{3/2}$ or $D_{5/2}$ level. The resonant vector or is not drawn, but is represented by a circle which is the locus of all possible end points of the t vector. The resultant scattering amplitude is the vector drawn from the origin to the head of the resonant vector, that is, to some point on the circle. For bombarding energies considerably below the resonant energy, the head of the resonant vector is near the head of the non-resonant vector through which the circle is drawn. As the energy increases, the head of the resonant vector moves counterclockwise around the circle. The journey is about half completed when the bombarding energy is equal to the resonant energy.

is only one-half the diameter of the $P_{3/2}$ circle so that the greatest possible maximum is much smaller.

$S_{1/2}D_{3/2}$ and $S_{3/2}D_{3/2}$

Figure 5 shows the general behavior of the resonance for the $S_{1/2}D_{3/2}$ combination. For definiteness, an arbitrary $S_{1/2}$ vector is shown, but the argument holds for any possible $S_{1/2}$ vector. As the potential phase shift of the $D_{3/2}$ wave is negligible, δ_{2-} is approximately zero below the resonance. When passing through the resonance in the direction of increasing energy, δ_{2-} increases from about 0° to some value near 180° . The $D_{3/2}$ vector consequently moves about the circle, successively passing points 1,

2, and 3. No matter how the $S_{1/2}$ vector misbehaves meanwhile, the minimum on the low-energy side of the maximum cannot be produced. The same argument also holds for the $S_{3/2}D_{3/2}$ case, since the only difference is an increase in the diameter of the D circle.

$P_{1/2}P_{1/2}$ and $P_{3/2}P_{3/2}$

Figure 6 applies to the $P_{1/2}P_{1/2}$ case. The R , $S_{1/2}$, and $P_{1/2}$ vectors and the $P_{1/2}$ circle are drawn together with the largest possible resultant. Including the incoherent part, the corresponding cross section is

$$(d\sigma/d\omega)_{\max} = 0.16 \text{ barn}$$

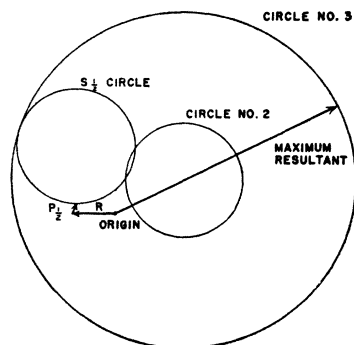


FIG. 4. The partial wave vectors at $E_p \sim 1.7$ Mev drawn on the assumption that the scattering anomaly at this energy is due to an $S_{1/2}$ level and a $P_{3/2}$ level closely spaced. The R and $P_{1/2}$ vectors are nearly constant over the region of the resonance. The $S_{1/2}$ circle is the locus of all possible end points of the $S_{1/2}$ vector. Circle No. 2 is the locus of all possible centers of the $P_{3/2}$ circle. It is the same diameter as the $S_{1/2}$ circle and is displaced from it by a distance equal to the radius of the $P_{3/2}$ circle. Circle No. 3 is the outer envelope of all possible $P_{3/2}$ circles. Since no part of any $P_{3/2}$ circle lies outside of Circle No. 3, the greatest possible scattering amplitude obtainable from an $S_{1/2}P_{3/2}$ combination is that shown in the figure.

which is impossibly small. Since the $P_{3/2}$ circle is smaller than the $P_{1/2}$ circle, the attainable maximum for the $P_{3/2}P_{1/2}$ case is even smaller. We note in passing that the $P_{1/2}$ circle is almost concentric with the origin so that, under the conditions of the experiment, a single $P_{3/2}$ resonance would have little visible effect on the experimental cross section. At the scattering angle employed, the incoherent part would produce a small maximum.

$P_{1/2}P_{3/2}$

Figure 7 shows the R and $S_{1/2}$ vectors, the $P_{3/2}$ circle, and the locus of centers of the $P_{3/2}$ circles. The large circle is the envelope of the $P_{3/2}$ circles. Even with the incoherent contribution, the maximum attainable cross

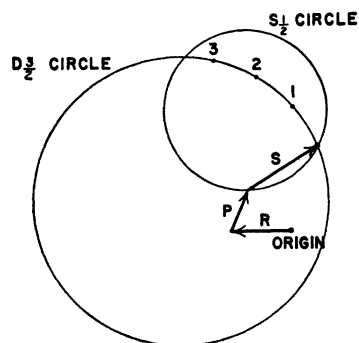


FIG. 5. The partial wave vectors at $E_p \sim 1.7$ Mev drawn on the assumption that the scattering anomaly at this energy is due to an $S_{1/2}$ and a $D_{3/2}$ resonance closely spaced. The P vector is the sum of the $P_{1/2}$ and $P_{3/2}$ vectors. The R and P vectors are nearly constant over the region of the resonance. The $S_{1/2}$ circle together with an arbitrary $S_{1/2}$ vector are shown. The position of the $D_{3/2}$ circle is determined by the vector S . The head of the $D_{3/2}$ vector lies on this circle, and as the energy increases, successively passes points 1, 2, and 3. The resultant scattering amplitude is the vector drawn from the origin to the head of the $D_{3/2}$ vector.

section is

$$(d\sigma/d\omega)_{\max} = 0.50 \text{ barn}$$

which is too small.

$P_{3/2}D_{3/2}$ and $P_{1/2}D_{3/2}$

Figure 8 shows the R , $S_{1/2}$, and $P_{3/2}$ vectors, the $P_{3/2}$ circle and a $D_{3/2}$ circle drawn for an arbitrary $P_{1/2}$ vector ending at point D . This figure also applies to the $P_{1/2}D_{3/2}$ case, the only difference being an increase in the diameter of the D circle. These combinations are ruled out by the following line of reasoning. To obtain the minimum on the low-energy side, the D vector must still be quite small when the $P_{3/2}$ vector reaches the point C . So the D vector is practically zero at all lower energies. Somewhere below the resonance, the $P_{3/2}$ vector is in the vicinity of point A . In approaching the resonance from the low-energy side, the head of the $P_{3/2}$ vector moves counterclockwise from point A , through

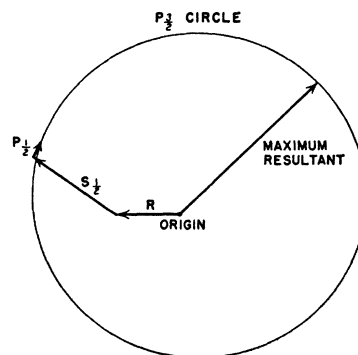


FIG. 6. The partial wave vectors at $E_p \sim 1.7$ Mev drawn on the assumption that the scattering anomaly at this energy is due to two $P_{3/2}$ levels closely spaced. This possibility differs from the assumption of a single $P_{3/2}$ level [Fig. 4(c)] only in that the phase shift δ_{l^+} is now a function of the parameters of both levels. As the energy is varied, the head of the $P_{3/2}$ vector will move in a complicated manner about the circle. The maximum scattering amplitude attainable is that shown in the figure.

point B , toward point C . In so moving, the resultant becomes monotonically smaller since the D vector cannot make an appreciable contribution in this range. The experimental curve, on the contrary, shows a small but unmistakable increase in the cross section just before the minimum, so these combinations are not satisfactory.

$P_{3/2}D_{3/2}$

This case differs from the $P_{1/2}D_{3/2}$ case only in that the diameter of the $D_{3/2}$ circle is one-third less than that of the $D_{3/2}$ circle. In fitting the $P_{3/2}D_{3/2}$ case, it was just possible to attain the experimental cross section and also reproduce the shape of the resonance. Efforts to attain substantially higher maxima cause unreasonable distortion of the curve. Because of the decreased size of the $D_{3/2}$ circle, the $P_{3/2}D_{3/2}$ combination cannot fit the experimental curve.

$D_{\frac{3}{2}}D_{\frac{3}{2}}$, $D_{\frac{3}{2}}D_{\frac{1}{2}}$, and $D_{\frac{1}{2}}D_{\frac{1}{2}}$

These combinations can be easily discarded. At this energy both D circles lie to the left of the head of the previously drawn vector as shown in Fig. 3(d). Thus, the smallest resultant obtainable is not very much smaller than the resultant of the R , $S_{\frac{3}{2}}$, $P_{\frac{3}{2}}$, and $P_{\frac{1}{2}}$ vectors alone. Since the cross section calculated from the sum of these vectors is much greater than the first minimum, none of these combinations is acceptable.†

IV. DISCUSSION

The $C^{12}(p,\gamma)N^{13}$ reaction has two observed resonances. One is at $E_p = 0.456 \pm 0.002$ Mev with $\Gamma = 35$ kev,¹⁰ and the other is at $E_p = 1.697 \pm 0.012$ Mev with $\Gamma = 74$ kev.¹¹

These values apply in the laboratory frame of reference, and E_p is the kinetic energy of the incident proton. The corresponding values in the center-of-mass system, with E_r measured from the ground state of N^{13} , are $E_r = 2.366$ Mev and $\Gamma = 32$ kev for the lower capture resonance, and $E_r = 3.510$ Mev and $\Gamma = 68$ kev for the other. The energy of the lower level as determined from the (p,γ) reaction differs from our value for the $S_{\frac{1}{2}}$ level by 13 kev. Part of the difference is probably due to the fact that Δ_λ is large (~ 1.4 Mev) and varies rapidly with k and a , thus making our value of E_r uncertain, but it is impossible to explain the entire discrepancy on this basis. Our analysis of the $S_{\frac{1}{2}}$ level gives a width at half maximum of 33 kev, which agrees with the capture data. Our value of $E_r = 3.501$ Mev for the $P_{\frac{3}{2}}$ level is within the experimental error quoted for the upper capture level, while our value of 3.549 Mev for the $D_{\frac{3}{2}}$ level is somewhat too high, indicating that most of the observed gamma-rays come from the $P_{\frac{3}{2}}$ level. This behavior is consistent with the assumption of a $P_{\frac{3}{2}}$ ground state for N^{13} since the $(P_{\frac{3}{2}}, P_{\frac{3}{2}})$ transition can occur by magnetic dipole or electric quadrupole radiation, and so should be much more probable than the $(D_{\frac{3}{2}}, P_{\frac{3}{2}})$ transition to the ground state which requires magnetic quadrupole or electric octopole radiation. However, the calculated widths of the $P_{\frac{3}{2}}$ and $D_{\frac{3}{2}}$ levels are only 42 and 40 kev, respectively, so that the large total width of 74 kev observed by Van Patter¹¹ possibly indicates that both levels participate in the capture process. One may also expect some 1.1-Mev gamma-radiation from the $(P_{\frac{3}{2}}, S_{\frac{3}{2}})$ electric dipole and the $(D_{\frac{3}{2}}, S_{\frac{3}{2}})$ electric quadrupole transitions. If such gamma-rays exist, their observation would lend support to the

† Note added in proof: In a private communication Dr. E. P. Wigner has recently informed us that the upper limit for γ_λ^2 should be twice the value given above. This increased value does not absolutely exclude the possibility of an F level at the upper scattering anomaly. However application of the techniques used above shows that neither a single F level nor an F level in combination with another can account for the observed cross section. Since a detailed consideration of these possibilities would necessarily be quite long, it is omitted.

¹⁰ W. A. Fowler and C. C. Lauritsen, Phys. Rev. **76**, 314 (1949).

¹¹ D. M. Van Patter, Phys. Rev. **76**, 1264 (1949).

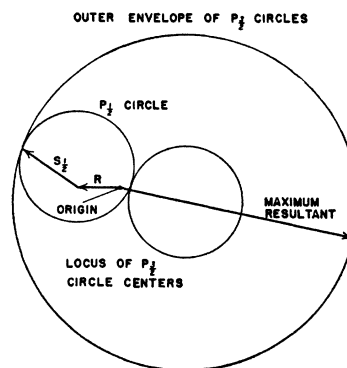


FIG. 7. The partial wave vectors at $E_p \sim 1.7$ Mev drawn on the assumption that the scattering anomaly at this energy is due to a $P_{\frac{3}{2}}$ and a $P_{\frac{1}{2}}$ level closely spaced. The R and $S_{\frac{3}{2}}$ vectors are nearly constant over the region of the resonance. The $P_{\frac{3}{2}}$ vector is replaced by its circle. The small circle to the right of the origin is the locus of centers of all possible $P_{\frac{3}{2}}$ circles and the large circle is their outer envelope. Since no part of any $P_{\frac{3}{2}}$ circle lies outside the outer envelope, the greatest possible scattering amplitude is that shown in the figure.

present level classification. However, their intensities may be quite weak on account of the relatively small energy differences between the $S_{\frac{3}{2}}$ and the $P_{\frac{3}{2}}$ and $D_{\frac{3}{2}}$ levels.

In addition to the C^{13} levels at 3.083 and 3.677 Mev,¹² Rotblat¹³ reports a level at 3.9 Mev. Assuming the equality of nn and pp forces, the existence of this level is consistent with the results of the present analysis.

Finally, the present level assignment supports Mayer's hypotheses¹⁴ of large spin-orbit coupling and level inversion in nuclei. According to her model, the

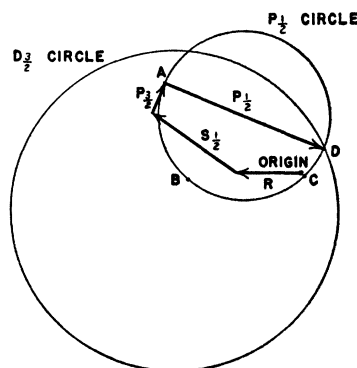


FIG. 8. The partial wave vectors at $E_p \sim 1.7$ Mev drawn on the assumption that the scattering anomaly at this energy is due to a $P_{\frac{3}{2}}$ and a $D_{\frac{3}{2}}$ level closely spaced. The R , $S_{\frac{3}{2}}$, and $P_{\frac{3}{2}}$ vectors are nearly constant over the region of the resonance. The $P_{\frac{3}{2}}$ circle together with an arbitrary $P_{\frac{3}{2}}$ vector is shown. When E_p is much less than the resonant energy for the $P_{\frac{3}{2}}$ level, the head of the $P_{\frac{3}{2}}$ vector is near point A. As the energy increases, the head of the $P_{\frac{3}{2}}$ vector successively passes points B, C, and D. The $D_{\frac{3}{2}}$ circle is drawn for the $P_{\frac{3}{2}}$ vector at point D. The head of the $D_{\frac{3}{2}}$ vector is somewhere on this circle and the resultant scattering amplitude is the vector drawn from the origin to the head of the $D_{\frac{3}{2}}$ vector.

¹² R. Malm and W. W. Buechner, Phys. Rev. **81**, 519 (1951).

¹³ J. Rotblat, Proc. Harwell Nuclear Physics Conference, September, 1950.

¹⁴ M. G. Mayer, Phys. Rev. **78**, 16 (1950).

unexcited N^{13} nucleus has two protons in the $1S_{\frac{1}{2}}$ shell, four protons in the $1P_{\frac{1}{2}}$ shell, and one proton in the $1P_{\frac{3}{2}}$ shell. The excited levels available to the outer proton are: $1D_{\frac{1}{2}}$, $1D_{\frac{3}{2}}$, $2S_{\frac{1}{2}}$, $1F_{\frac{1}{2}}$, $1F_{\frac{3}{2}}$, $2P_{\frac{1}{2}}$, $2P_{\frac{3}{2}}$; etc. On the basis of the present analysis, the $D_{\frac{1}{2}}$ and $P_{\frac{1}{2}}$ levels appear at about 3.5 Mev while the $D_{\frac{3}{2}}$ and $P_{\frac{3}{2}}$ levels presumably lie above 5.6 Mev, since experiment shows no other scattering anomalies below this energy. So, it appears that these doublets are inverted and the splitting is large.[§]

§ *Note added in proof:* In the single particle approximation the reduced widths of the energy levels are approximately equal to $\hbar^2/\mu a$. (See reference 4.) On the basis of this analysis, the reduced widths of the $S_{\frac{1}{2}}$, $P_{\frac{1}{2}}$, and $D_{\frac{1}{2}}$ levels are 82 percent, 4.1 percent, and 24 percent of this value, respectively. The relatively small width of the $P_{\frac{1}{2}}$ level indicates that it is not a single particle level but

It is possible that one or more levels of high angular momentum or very small reduced width lie below 5.64 Mev, even though none was observed.² In the single-level approximation, the width of any level is inversely proportional to A_l^2 which increases rapidly with l . As the elastic scattering cross section was measured at 30-kev intervals away from the observed anomalies, such a level could have escaped detection.

We are most grateful to Dr. H. T. Richards for his interest, encouragement, and counsel throughout this undertaking, and to Dr. R. K. Adair and Dr. and Mrs. R. A. Laubenstein for information and advice.

rather arises from the excitation of two or more nucleons. If such is the case, the above argument does not apply so far as the $P_{\frac{3}{2}}$ level is concerned.

PHYSICAL REVIEW

VOLUME 84, NUMBER 3

NOVEMBER 1, 1951

The Molecular Structure of Methyl Alcohol

DONALD G. BURKHARD* AND DAVID M. DENNISON

Harrison M. Randall Laboratory of Physics, University of Michigan, Ann Arbor, Michigan

(Received May 28, 1951)

A qualitative discussion of the near and far infrared spectrum of methyl alcohol shows that the rotational states, including the hindered rotation, may be well represented by a model consisting of a rigid hydroxyl and a rigid methyl group. These groups may perform a mutual rotation with respect to each other about the symmetry axis of the methyl group subject to a hindering potential which is assumed to have the form $V = \frac{1}{2}H(1 - \cos 3x)$ where x is the angle of mutual rotation. A series of lines in the microwave spectrum, discovered by Hershberger and Turkevich, have recently been measured with great accuracy by Coles who also determined their Stark splitting. The positive identification of these lines leads at once to an estimate of the barrier height H .

The wave equation for the rotation of methyl alcohol is obtained and the matrix elements of the hamiltonian are evaluated using the wave functions derived by Koehler and Dennison on the basis of a simplified model. Diagonalizing the hamiltonian yields

the energy levels which are found to predict correctly the principal features of the microwave spectrum. A quantitative comparison serves to fix the moments and product of inertia to have the values, $A = 34.28$, $C_1 = 1.236$ and $D = -0.107$ all times 10^{-40} g cm². The two components of the electric moment are determined, $\mu_{11} = 0.893$ and $\mu_{12} = 1.435 \times 10^{-18}$ esu. A relation is obtained between the barrier height H and the moment of inertia C_2 of the methyl group about its symmetry axis. Assuming C_2 to be equal to the methane moment of inertia, then $H = 380$ cm⁻¹. If, in addition to taking a methane-like structure for the methyl group, it is assumed that the OH distance is the same as in water, namely 0.958A, one finds that (1) the CO distance is 1.421A, (2) the symmetry axis of the methyl group lies between the O and H atoms with the O displaced 0.084A from it and (3) the COH bond angle is 110° 15'. This latter angle is 5° 44' greater than the apex angle in water vapor.

INTRODUCTION

THE spectrum of methyl alcohol has been examined by a number of investigators. The region from 2.5μ to 26μ was mapped by Borden and Barker¹ and the principal fundamental vibration frequencies were identified. The spectrum from 20μ to 57μ was measured by Lawson and Randall² who found it to consist of an intense series of irregularly but closely spaced lines. These are undoubtedly connected with the torsional vibration or hindered rotation of the molecule. More recently the microwave spectrum has been explored. A series of lines around 25,000 Mc which, from the regularity of their spacing, must clearly have a common

origin, were discovered by Hershberger and Turkevich.³ These lines were also observed by Dailey⁴ and later were remeasured with high precision by Coles.⁵ Coles not only found many more members of the series but also determined the number and spacing of the Stark components. Edwards, Gilliam, and Gordy⁶ have measured a number of lines between 50,000 Mc and 35,000 Mc.

The general structure of methyl alcohol is fairly well known from chemical and spectroscopic evidence and is shown in Fig. 1. The methyl group is presumably very similar to the methyl group in methane or in the methyl

* Now at the Department of Physics, University of Colorado, Boulder, Colorado.

¹ A. Borden and E. F. Barker, *J. Chem. Phys.* **6**, 553 (1938).

² J. R. Lawson, thesis, University of Michigan (1938).

³ W. D. Hershberger and J. Turkevich, *Phys. Rev.* **71**, 554 (1947).

⁴ B. P. Dailey, *Phys. Rev.* **72**, 84 (1947).

⁵ D. K. Coles, *Phys. Rev.* **74**, 1194 (1948).

⁶ Edwards, Gilliam, and Gordy (to be published). We are very much indebted to Professor Gordy for sending us a preliminary account of their work.